Comparative diagnostic performance of volumetric laser endomicroscopy and confocal laser endomicroscopy in the detection of dysplasia associated with Barrett's esophagus

Cadman L. Leggett, MD[1], **Emmanuel C. Gorospe, MD**[1], **Daniel K. Chan, MD**[1], **Prasuna Muppa, MD**[1], **Victoria Owens, MD**[2], **Thomas C. Smyrk, MD**[2], **Marlys Anderson, BS**[1], **Lori S. Lutzke, CCRP**[1], **Guillermo Tearney, MD**[3], and **Kenneth K. Wang, MD**[1]

Rochester, Minnesota, USA

Abstract

Background and Aims—Probe-based confocal laser endomicroscopy (pCLE) and volumetric laser endomicroscopy (VLE) (also known as frequency domain optical coherence tomography) are advanced endoscopic imaging modalities that may be useful in the diagnosis of dysplasia associated with Barrett's esophagus (BE). We performed pCLE examination in ex-vivo EMR specimens and compared the diagnostic performance of using the current VLE scoring index (previously established as OCT-SI) and a novel VLE diagnostic algorithm (VLE-DA) for the detection of dysplasia.

Methods—A total of 27 patients with BE enrolled in a surveillance program at a tertiary-care center underwent 50 clinically indicated EMRs that were imaged with VLE and pCLE and classified into neoplastic (N = 34; high-grade dysplasia, intramucosal adenocarcinoma) and nonneoplastic (N = 16; low-grade dysplasia, nondysplastic BE), based on histology. Image datasets (VLE, N = 50; pCLE, N = 50) were rated by 3 gastroenterologists trained in the established diagnostic criteria for each imaging modality as well as a new diagnostic algorithm for VLE derived from a training set that demonstrated association of specific VLE features with neoplasia. Sensitivity, specificity, and diagnostic accuracy were assessed for each imaging modality and diagnostic criteria.

Results—The sensitivity, specificity, and diagnostic accuracy of pCLE for detection of BE dysplasia was 76% (95% confidence interval [CI], 59–88), 79% (95% CI, 53–92), and 77% (95% CI, 72–82), respectively. The optimal diagnostic performance of OCT-SI showed a sensitivity of 70% (95% CI, 52–84), specificity of 60% (95% CI, 36–79), and diagnostic accuracy of 67%; (95% CI, 58–78). The use of the novel VLE-DA showed a sensitivity of 86% (95% CI, 69–96), specificity of 88% (95% CI, 60–99), and diagnostic accuracy of 87% (95% CI, 86–88). The diagnostic accuracy of using the new VLE-DA criteria was significantly superior to the current OCT-SI (*P* < .01).

Conclusion—The use of a new VLE-DA showed enhanced diagnostic performance for detecting BE dysplasia ex vivo compared with the current OCT-SI. Further validation of this algorithm in vivo is warranted.

Barrett's esophagus (BE) is the strongest risk factor for the development of esophageal adenocarcinoma, a disease with rising incidence in the United States.[1] Detection of dysplasia associated with BE is of critical importance in determining the risk of progression to cancer and need for endoscopic ablation therapy. Advanced imaging techniques have been shown to significantly increase detection of dysplasia and in some studies reduce the number of suggested biopsies in patients with BE.[2]

Confocal laser endomicroscopy (CLE) is an optical imaging modality that can generate in vivo images of esophageal mucosa at histologic level resolution. The use of probe-based confocal laser endomicroscopy (pCLE) has been shown to enhance detection of BE-associated dysplasia compared with high-definition white-light endoscopy alone.[3] pCLE, however, has limited imaging depth and a very limited field of view. In addition, pCLE requires administration of intravenous fluorescent contrast agents in order to visualize the esophageal mucosa.

Frequency domain optical coherence tomography imaging, also known as volumetric laser endomicroscopy (VLE), is a second-generation optical coherence tomography (OCT) device that, in conjunction with a balloon-imaging catheter, can generate wide-field cross-sectional views of the entire distal portion (4–6 cm) of the human esophagus. VLE allows for comprehensive assessment of the esophageal mucosa and submucosa; however, its lateral resolution of about 30 μm is approximately 10 times lower than that of pCLE. VLE can effectively distinguish normal squamous epithelium from BE and uses an established OCT scoring index (OCT-SI) to detect dysplasia.[4,5]

pCLE and VLE have unique advantages and disadvantages for the detection of dysplasia associated with BE. This study aims to compare the diagnostic performance of VLE and pCLE by using their respective diagnostic criteria for BE dysplasia. In addition, we introduce and perform preliminary validation of a novel diagnostic algorithm designed for VLE.

METHODS

Patient and EMR specimens

EMR specimens were obtained from patients enrolled in a tertiary-care BE unit at Mayo Clinic, Rochester Minnesota. The patients consented to participate in this study. All patients had a history of high-grade dysplasia (HGD) or intra-mucosal adenocarcinoma (IMC). Endoscopic resection was performed by a single endoscopist (K.K.W.) with experience in the endoscopic management of BE, by using either the cap-snare (Olympus USA, Center Valley, Pa) or the band-ligation technique (Wilson-Cook Medical, Winston-Salem, NC).[6] This study was approved by the Mayo Clinic Institutional Review Board.

Specimen processing

In this study, EMR specimens were used as a tissue platform to establish a direct correlation between pCLE, VLE, and histology. Immediately after endoscopic resection, the specimens were rinsed with phosphate-buffered saline solution, oriented along the longitudinal axis, and marked with an ink dot on the lateral margin at the 12 o'clock position. VLE imaging was performed on each individual EMR specimen by using the Nvision VLE imaging system (Nvision, Cambridge, Mass). Specimens were then incubated in 0.5 μM 2-[N-(7-nitrobenz-2-oxa-1,3-diaxol-4-yl) amino]-2-deoxyglucose (2-NBDG) for 20 minutes at room temperature as previously described.[7] This agent supplies fluorescent contrast to dysplastic cells being incorporated through the glucose transporter. After the incubation period, the specimens were rinsed with phosphate buffered saline solution and imaged by using pCLE (Cellvizio, Mauna Kea Technologies, Paris, France). All EMR specimens were submitted for histopathologic evaluation by a GI pathologist (T.C.S., V.O.) for the presence and extent of dysplasia. (Fig. 1).

Specimens were considered neoplastic if the highest grade of dysplasia contained in the EMR specimen was HGD or IMC. Given that the diagnostic performance of both pCLE and VLE are limited in their differentiation of low-grade dysplasia (LGD), EMR specimens were grouped as nonneoplastic if they contained either nondysplastic BE or focal LGD.

Image acquisition and selection

The Nvision VLE imaging system used in this study consisted of a console, monitor, and optical probe. The optical probe is designed to fit through a therapeutic endoscope's instrument channel (3.7 mm). The probe used in this study is centered by a 25-mm balloon that is 6 cm in length. Imaging is performed by automatic helical pullback of the probe from the distal to the proximal end of the balloon over 90 seconds. VLE images have an axial resolution of 7 μm, a transverse resolution of about 30 mm, and can reach an imaging depth of up to 2 to 3 mm. A total of 1200 cross-sectional images are acquired over a 6-cm VLE scan. VLE scans are viewed by using a software interface that allows simultaneous examination of cross-sectional transverse and longitudinal views. In this study, VLE imaging was performed by direct application of the VLE balloon over the EMR specimen oriented along its longitudinal axis with gentle pressure to avoid distortion of EMR specimen structures.

The pCLE imaging system used in this study consists of a console, monitor, and optical probe. The optical probe used was a high-definition probe (Gastroflex UHD, Mauna Kea Technologies, Paris, France) designed to fit through a diagnostic gastroscope's instrument channel. pCLE has a field of view of 240 μm, with a lateral resolution of <5 μm. In our study, the pCLE image probe was stabilized by using a mechanical probe holder adapted over a translational mechanical stage as previously described.[7] Orientation of EMR specimens was preserved along the longitudinal axis, and pCLE videos were captured at a rate of 12 frames per second in a grid scanning pattern across the entire surface area of each specimen.

pCLE and VLE image acquisition was performed by 2 authors (C.L.L., M.A.) who reviewed videos and scans for image quality while remaining blinded to histology.

CLE fluorescence criteria

The CLE fluorescence intensity criteria were developed for the detection of BE-associated dysplasia by using 2-NBDG as a fluorescent agent in EMR specimens.[7] The components of these criteria are described in Figure 2. These criteria have been reported to have a sensitivity of 74% and specificity of 86% in the diagnosis of dysplasia in BE.[7]

OCT-SI

The OCT-SI is a scoring index previously validated for detection of dysplasia in BE.[5] The components of the OCT-SI are summarized in Figure 3. An OCT-SI dysplasia score of 2 has been associated with a sensitivity of 83% and a specificity of 75% for the diagnosis of neoplasia in BE by using OCT.[5]

VLE-DA

An independent training set of 30 EMR VLE scans was examined by 2 investigators (C.L.L., E.C.G.) for features associated with dysplasia. Based on the identified features of atypical gland counts and effacement of the VLE mucosal layer (Fig. 4), a new VLE diagnostic algorithm (VLE-DA) (Fig. 5) was generated and analyzed to determine its diagnostic performance. Information on the development of the VLE-DA is provided in the supplemental section of the publication (Supplemental text, available online at www.giejournal.org).

When established criteria are used, OCT can distinguish BE from squamous and gastric epithelium (sensitivity = 85%, specificity = 95%).[4,8,9] Once BE is identified, the VLE-DA is interpreted over one longitudinal centimeter of BE mucosa (mean longitudinal distance of EMR specimen in training set). The VLE-DA is first used to distinguish the degree of VLE mucosal layer effacement. Effacement of the VLE mucosal layer refers to the partial or complete loss of the layered mucosal architecture observed with squamous epithelium. Compared with squamous epithelium, a partially effaced VLE mucosal layer provides less distinction between mucosa and submucosa, often containing several breaks.

Partial effacement of the VLE mucosal layer was defined by a mucosal layer 2 mm (mean length of mucosal layer measured) in transverse cross-sectional length present in 50% of a 1-cm longitudinal scan. Once a partially effaced VLE mucosal layer is identified, the VLE-DA requires the rater to perform quantification of atypical glands. Atypical VLE glands are cystic structures that have an irregular shape and size. The presence of >5 atypical glands over 1 longitudinal centimeter was rated as neoplastic.

Complete effacement of the mucosal layer was defined by absence of a mucosal layer or its presence in <2 mm in transverse cross-section over <50% of the scan. If complete effacement of the mucosal layer is present, the VLE-DA requires the rater to interpret the most prevalent surface-to- subsurface intensity ratio (surface > subsurface intensity vs surface subsurface intensity) present in 50% of the scan. A rating of surface intensity

greater than subsurface intensity is considered neoplastic. Rating of surface-to- subsurface intensity was reserved for scans with complete effacement of the mucosal layer because partial effacement could potentially be misinterpreted as surface less than subsurface intensity.

Retrospective analysis of the VLE-DA by using the training set showed a sensitivity and specificity of 83% (95% confidence interval [CI], 58–96) and 79% (95% CI, 49–94), respectively.[10]

Rater training and validation dataset rating

Three gastroenterologists with experience in advanced imaging in BE (C.L.L., E.C.G., D.K.C.) served as reviewers for the VLE and pCLE validation datasets. All raters were provided with a training session for pCLE and VLE, respectively, followed by a brief examination. The pCLE training session consisted of a 30-minute presentation including 15 sample pCLE single-plane images rated by using the pCLE fluorescence intensity criteria. The VLE training session consisted of a 30-minute presentation including 15 sample VLE single-plane images rated by using the OCT- SI and the VLE-DA. A set of 15 pCLE and 15 VLE images were used to test the reviewers' level of proficiency for each criteria. Raters were expected to score >85% before proceeding with scoring of the VLE (by using OCT-SI, VLE-DA) and pCLE validation datasets.

Reviewers were blinded to patient history, endoscopic findings, and histopathology diagnoses. For pCLE videos, reviewers were asked to independently rate each video in the validation set as (1) neoplastic or (2) nonneoplastic by using the pCLE fluorescent criteria. For VLE scans, reviewers were asked to provide scoring for surface intensity (0, 1, 2) and glandular architecture (0, 1,2), and a dysplasia score was subsequently calculated by adding the 2 scores. After a period of washout (1 month) to limit visual recognition of images from rating by using the OCT-SI, reviewers were presented with a re-randomized test image dataset and asked to use the VLE-DA to rate scans as (1) neoplastic versus (2) nonneoplastic. Reviewers were unaware of the results of their previous rating.

Statistical analyses

Based on the study of Gaddam et al[11] for validating the interobserver agreement and accuracy of probe-based endomicroscopy, at least 30 images are required to have a power of 80% to detect reasonable effect size ($\alpha = 0.05$). Measures of diagnostic performance, including sensitivity, specificity, positive predictive value, negative predictive value, and diagnostic accuracy for pCLE and VLE by using established and new diagnostic scoring indices were obtained by using the JMP statistical package (SAS Institute, Cary, NC). Agreement among the 3 raters was assessed by using a multiple-rater kappa statistic.[12] Level of agreement was determined by using the Landis and Koch standards for the following kappa coefficients: 0 = poor, 0.01 to 0.20 = slight, 0.21 to 0.40 = fair, 0.41 to 0.60 = moderate, 0.61 to 0.80 = substantial, and 0.81 to 1 = almost perfect.[13] Paired nominal data from OCT-SI and VLE-DA were assessed for marginal homogeneity by using the McNemar test.

RESULTS

Baseline characteristics

The final validation dataset used in this study consisted of 50 EMR specimens obtained from 27 patients, with an average number of 1.8 EMR specimens per patient (range 1–7). Patient and histologic characteristics are summarized in Table 1. The average (± standard deviation [SD]) EMR specimen length, width, and height were 0.9 (± 0.2), 0.6 (± 0.1), and 0.3 (± 0.1) cm, respectively. Of 50 EMR specimens, 16 (32%) were considered nonneoplastic (nondysplastic BE, N = 10; LGD, N = 6) and 34 (68%) neoplastic (HGD, N = 24; IMC, N = 10).

Diagnostic performance

When histopathology was used as the criterion standard, pCLE showed a sensitivity of 76% (95% CI, 59–88), a specificity of 79% (95% CI, 53–92), and a diagnostic accuracy of 77% (95% CI, 72–82) for BE-associated dysplasia. VLE scans evaluated by using the OCT-SI showed a sensitivity of 93% (95% CI, 78–98), specificity of 18% (95% CI, 7–44), and a diagnostic accuracy of 69% (95% CI, 62–84) at a dysplasia threshold of 2. Analysis also was performed for the OCT-SI at various thresholds (Supplemental Table 1, available online at www.giejournal.org). A threshold of 3 showed improved diagnostic characteristics compared with other thresholds, with a sensitivity of 70% (95% CI, 52–84), specificity of 60% (95% CI, 36–79), and diagnostic accuracy of 67% (95% CI, 58–78). VLE scans rated by using the VLE-DA showed a sensitivity of 86% (95% CI, 69–95), specificity 88% (95% CI, 61–98), and diagnostic accuracy of 87% (95% CI, 86–88). The diagnostic accuracy of the VLE- DA was significantly superior to the diagnostic accuracy of the OCT-SI at a dysplasia threshold of 3 ($P < .01$).

A summary of the diagnostic performance of pCLE and VLE in differentiating dysplasia associated with BE is shown in Figure 6.

Intraobserver and interobserver agreement

Interrater agreement was fair, with OCT-SI (kappa 0.39), moderate with pCLE (kappa 0.46), and substantial for VLE- DA (kappa 0.83).

DISCUSSION

This study compares the diagnostic performance of VLE and pCLE and introduces a new diagnostic algorithm designed to distinguish neoplastic BE by using VLE.

The diagnostic performance of pCLE in our study (sensitivity 76%, specificity 79%, and diagnostic accuracy 77%) was similar to that of a previous study published by our group that imaged EMR specimens by using an endoscope-based CLE system (sensitivity 74%, specificity 86%, diagnostic accuracy 78%).[7] The lower specificity observed in the current study can be attributed to differences in methodology between studies (pCLE videos versus single plane images). Although pCLE videos allowed us to perform a comprehensive evaluation of the entire surface of the EMR specimen, this approach can lead to

interpretation bias if a rating of neoplasia is reached based on the interpretation of a few frames concerning for neoplasia despite overall characteristics of nonneoplastic BE.

VLE scans were interpreted by using a scoring index developed and validated for detection of neoplasia by using a first-generation form of OCT. The diagnostic performance for VLE was analyzed at various dysplasia score thresholds. A dysplasia score of 2 has been previously associated with a sensitivity of 83% and a specificity of 75% in the detection of neoplasia, with OCT in vivo.[5] In our study, a dysplasia threshold of 3 showed optimal diagnostic characteristics (sensitivity 70%, specificity 60%, and diagnostic accuracy 67%) compared with other scores. The increased OCT-SI dysplasia threshold required for VLE may be attributed to the fact that the OCT-SI was developed by using a first-generation form of OCT that is different from VLE, which uses second-generation OCT technology and a balloon catheter.[5,14] Furthermore, compared with OCT used in prior studies in which single, about 5-mm wide images were used for diagnosis, image interpretation with the use of VLE is performed over a much wider field of view (6 cm, 1200 frames) that may have frame-to-frame variation in surface signal intensity. By using today's VLE, it is therefore uncommon for a rater to provide a surface intensity score of 0 (surface intensity < subsurface intensity), and therefore, the presence of any glandular structure would cause the scoring index to exceed the threshold for neoplasia diagnosis.

Owing to the limitations of applying first-generation OCT criteria (OCT-SI) to today's VLE images, we analyzed VLE data and histology from a training set of EMR specimens to develop a new VLE-DA for dysplasia in BE. In addition to the OCT-SI metric of surface-to-subsurface intensity, we identified partial effacement of the mucosal layer and number of atypical glandular structures as salient characteristics associated with dysplasia in BE by using VLE. The use of the VLE-DA showed improvement in diagnostic performance (sensitivity 86%, specificity 87%, and diagnostic accuracy 87%) compared with the previously established OCT-SI. Although the VLE-DA were validated by using an ex vivo EMR platform, it potentially can be adapted for in vivo VLE interpretation by using the image viewer region of interest (8×6 mm magnified view on image software) over a 1-cm longitudinal distance of BE mucosa. Interpretation can be performed systematically in 4 quadrants over the entire BE length.[15]

Ex vivo imaging of EMR specimens allowed us to perform direct correlation between pCLE, VLE, and histology. Although this practice provided us with high-quality images for interpretation, it does not represent image acquisition during endoscopy. In our study, this is especially true for pCLE in which the imaging probe was stabilized to obtain videos across the whole surface of the EMR specimen, allowing us to perform comprehensive pCLE imaging. Although the use of a topical fluorescent agent (2-NBDG) has been validated for detection of BE dysplasia in EMR specimens, this approach may not represent in vivo imaging using intravenous fluorescein.[7]

Advanced imaging modalities including pCLE and VLE have not been validated for detection of LGD in BE. The validation dataset in this study contained a total of 6 EMR specimens (12%) with LGD that were categorized as nonneoplastic. Emerging literature suggests that a subset of patients with LGD carry a high rate of neoplastic progression and

may benefit from endoscopic therapy.[16,17] We performed a subset analysis that categorized LGD EMR specimens as neoplastic. (Supplemental Table 2, available online at www.giejournal.org). A slight increase in sensitivity (pCLE 71% [95% CI, 55–83]; OCT-SI 68% [95% CI, 52–81]; VLE-DA 77% [95% CI, 60–88]) and decrease in specificity (pCLE 90% [95% CI, 54–98] ; OCT-SI 70% [95% CI, 38–89]; VLE-DA 93% [95% CI, 58–99]) was noted across imaging modalities, likely secondary to an enriched neoplastic dataset. Differences in diagnostic performance between imaging modalities, however, remained largely unchanged.

Our study design limits our ability to provide further insight into the histologic characteristics associated with the VLE features described. Histologic studies performed in esophagectomy specimens of patients with BE- associated adenocarcinoma have shown that areas of dysplasia are associated with replacement of the lamina propria with collagen-rich fibrotic tissue.[18–21] The high index of reflection of collagen (1.41–1.44) is associated with a more intense VLE signal. Although we are unaware of prior studies that quantify the distribution and degree of collagen in the lamina propria across the BE metaplasia-dysplasia-carcinoma sequence, it is possible that collagen content and distribution may account for the observed effacement of the mucosal layer from non- dysplastic to dysplastic BE. An increase in microvascular density also has been described across the metaplasia- dysplasia-carcinoma sequence, potentially contributing to the observed phenomenon.[22] Histologic studies also have described dilated ducts and glands that are surrounded, compressed, and deformed by a fibrotic lamina propria.[20,21] These cystic structures are thought to arise from compression of their glandular outlets by the collagen-rich tissue or by proliferating dysplastic cells. Their role in the pathogenesis of BE is not well- understood.

Finally, the effect of endoscopic ablation on the observed VLE features of mucosal layer effacement and atypical glandular structures is not completely understood. A recent study that used VLE to detect subsquamous esophageal structures after radio frequency ablation suggests that the prevalence of buried metaplasia under neosquamous epithelium is likely lower than previously estimated.[19] The effect of radio frequency ablation on VLE mucosal layer effacement has not been studied. Our study cohort included a total of 6 patients (22%) previously treated with radio frequency ablation. A subset analysis of the excluded EMR specimens (N = 9) from these patients showed no significant changes in diagnostic performance between imaging modalities (Supplemental Table 3, available online at www.giejournal.org).

Advanced imaging techniques such as pCLE and VLE may help in the diagnosis of dysplasia associated with BE. Although pCLE has better lateral resolution compared with VLE, VLE allows for rapid cross-sectional imaging of the entire luminal organ and provides information on various morphologic features. VLE also offers assessment of the entire BE segment and does not require a fluorescent contrast dye for its use. The diagnosis of BE-associated dysplasia with VLE has not yet been optimized because the current diagnostic scoring index was formulated and tested using an earlier form of OCT technology. We designed and performed preliminary validation of a VLE-DA that showed enhanced diagnostic performance compared with OCT-SI and pCLE. Further validation of this algorithm is necessary before its use is incorporated into clinical practice.

Supplementary Material

Refer to Web version on PubMed Central for supplementary material.

Acknowledgments

Abbreviations

2-NBDG	2-[N-(7-nitrobenz-2-oxa-1,3-diaxol-4-yl)amino]-2-deoxyglucose
BE	Barrett's esophagus
CLE	probe confocal laser endomicroscopy
HGD	high-grade dysplasia
IMC	intramucosal adenocarcinoma
LGD	low-grade dysplasia
OCT	optical coherence tomography
OCT-SI	volumetric laser endomicroscopy scoring index
pCLE	probe confocal laser endomicroscopy
VLE	volumetric laser endomicroscopy
VLE-DA	volumetric laser endomicroscopy diagnostic algorithm

References

1. Pohl H, Welch HG. The role of overdiagnosis and reclassification in the marked increase of esophageal adenocarcinoma incidence. J Natl Cancer Inst. 2005; 97:142–6. [PubMed: 15657344]

2. Qumseya BJ, Wang H, Badie N, et al. Advanced imaging technologies increase detection of dysplasia and neoplasia in patients with Barrett's esophagus: a meta-analysis and systematic review. Clin Gastroenterol Hepatol. 2013; 11:1562–1570. e1–2. [PubMed: 23851020]

3. Sharma P, Meining AR, Coron E, et al. Real-time increased detection of neoplastic tissue in Barrett's esophagus with probe-based confocal laser endomicroscopy: final results of an international multicenter, prospective, randomized, controlled trial. Gastrointest Endosc. 2011; 74:465–72. [PubMed: 21741642]

4. Sauk J, Coron E, Kava L, et al. Interobserver agreement for the detection of Barrett's esophagus with optical frequency domain imaging. Dig Dis Sci. 2013; 58:2261–5. [PubMed: 23508980]

5. Evans JA, Poneros JM, Bouma BE, et al. Optical coherence tomography to identify intramucosal carcinoma and high-grade dysplasia in Barrett's esophagus. Clin Gastroenterol Hepatol. 2006; 4:38–43. [PubMed: 16431303]

6. Gorospe EC, Leggett CL, Uno K, et al. Diagnosing dysplasia in Barrett's esophagus using volumetric laser endomicroscopy: submucosal gland characteristics. Am J Gastroenterol. 2013; 108:S32.

7. Gorospe EC, Leggett CL, Sun G, et al. Diagnostic performance of two confocal endomicroscopy systems in detecting Barrett's dysplasia: a pilot study using a novel bioprobe in ex vivo tissue. Gastrointest Endosc. 2012; 76:933–8. [PubMed: 22980290]

8. Evans JA, Bouma BE, Bressner J, et al. Identifying intestinal metaplasia at the squamocolumnar junction by using optical coherence tomography. Gastrointest Endosc. 2007; 65:50–6. [PubMed: 17137858]

9. Poneros JM, Brand S, Bouma BE, et al. Diagnosis of specialized intestinal metaplasia by optical coherence tomography. Gastroenterology. 2001; 120:7–12. [PubMed: 11208708]

10. Leggett CL, Gorospe EC, Chan DK, et al. Design and validation of new diagnostic criteria for dysplasia in Barrett's esophagus using volumetric laser endomicroscopy [abstract]. Gastrointest Endosc. 2014; 79:AB459–60.

11. Gaddam S, Mathur SC, Singh M, et al. Novel probe-based confocal laser endomicroscopy criteria and interobserver agreement for the detection of dysplasia in Barrett's esophagus. Am J Gastroenterol. 2011; 106:1961–9. [PubMed: 21946283]

12. Randolph, JJ. Free-marginal multirater kappa (multirater κfree): an alternative to Fleiss' fixed-marginal multirater kappa; Paper presented at University of Joensuu Learning and Instruction Symposium; October 14–15 2005; Joensuu, Finland.

13. Landis JR, Koch GG. The measurement of observer agreement for categorical data. Biometrics. 1977; 33:159–74. [PubMed: 843571]

14. Suter MJ, Vakoc BJ, Yachimski PS, et al. Comprehensive microscopy of the esophagus in human patients with optical frequency domain imaging. Gastrointest Endosc. 2008; 68:745–53. [PubMed: 18926183]

15. Leggett C, Chan D, Gorospe E, et al. Diagnostic performance of in-vivo volumetric laser endomicroscopy for detection of Barrett's esophagus dysplasia [abstract]. Gastrointest Endosc. 2015; 81:AB502.

16. Small AJ, Araujo JL, Leggett CL, et al. Radiofrequency ablation is associated with decreased neoplastic progression in patients with Barrett's esophagus and confirmed low-grade dysplasia. Gastroenterology. 2015; 149:567–76. [PubMed: 25917785]

17. Phoa KN, van Vilsteren FG, Weusten BL, et al. Radiofrequency ablation vs endoscopic surveillance for patients with Barrett esophagus and low-grade dysplasia: a randomized clinical trial. JAMA. 2014; 311:1209–17. [PubMed: 24668102]

18. Gray NA, Odze RD, Spechler SJ. Buried metaplasia after endoscopic ablation of Barrett's esophagus: a systematic review. Am J Gastroenterol. 2011; 106:1899–908. quiz 1909. [PubMed: 21826111]

19. Swager AF, Boerwinkel DF, de Bruin DM, et al. Detection of buried Barrett's glands after radiofrequency ablation with volumetric laser endomicroscopy. Gastrointest Endosc. Epub. 2015 Jun 26.

20. Rubio CA, Aberg B. Further studies on the musculo-fibrous anomaly of the Barrett's mucosa in esophageal carcinomas. Pathol Res Pract. 1991; 187:1009–13. [PubMed: 1792182]

21. Rubio CA, Riddell R. Musculo-fibrous anomaly in Barrett's mucosa with dysplasia. Am J Surg Pathol. 1988; 12:885–9. [PubMed: 3189695]

22. Konda VJ, Hart J, Lin S, et al. Evaluation of microvascular density in Barrett's associated neoplasia. Mod Pathol. 2013; 26:125–30. [PubMed: 22918163]
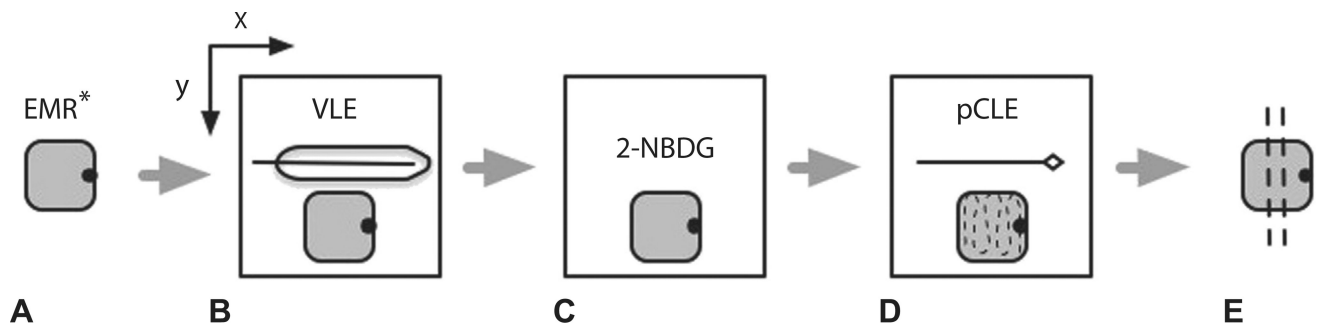
Figure 1.
Schematic representation of steps involved in imaging acquisition. **A**, EMR* specimen is marked for orientation. EMR specimen is placed on a holder attached to a translational mechanical stage that allows for movement in the x and y planes. **B**, EMR specimen is imaged with volumetric laser endomicroscopy. **C**, EMR specimen is incubated in 0.5 μM 2-[N-(7-nitrobenz-2-oxa-1,3-diaxol-4-yl)amino]-2-deoxyglucose for 20 minutes. **D**, EMR specimen is imaged with probe confocal laser endomicroscopy in video format across the entire surface area of the specimen in a grid scanning pattern. **E**, EMR specimen is placed in formalin and submitted for histologic sectioning. EMR and imaging probes not to scale. *VLE*, volumetric laser endomicroscopy; *2-NBDG*, 2-[N-(7-nitrobenz-2-oxa-1,3-diaxol-4-yl)amino]-2-deoxyglucose; *pCLE*, probe confocal laser endomicroscopy.
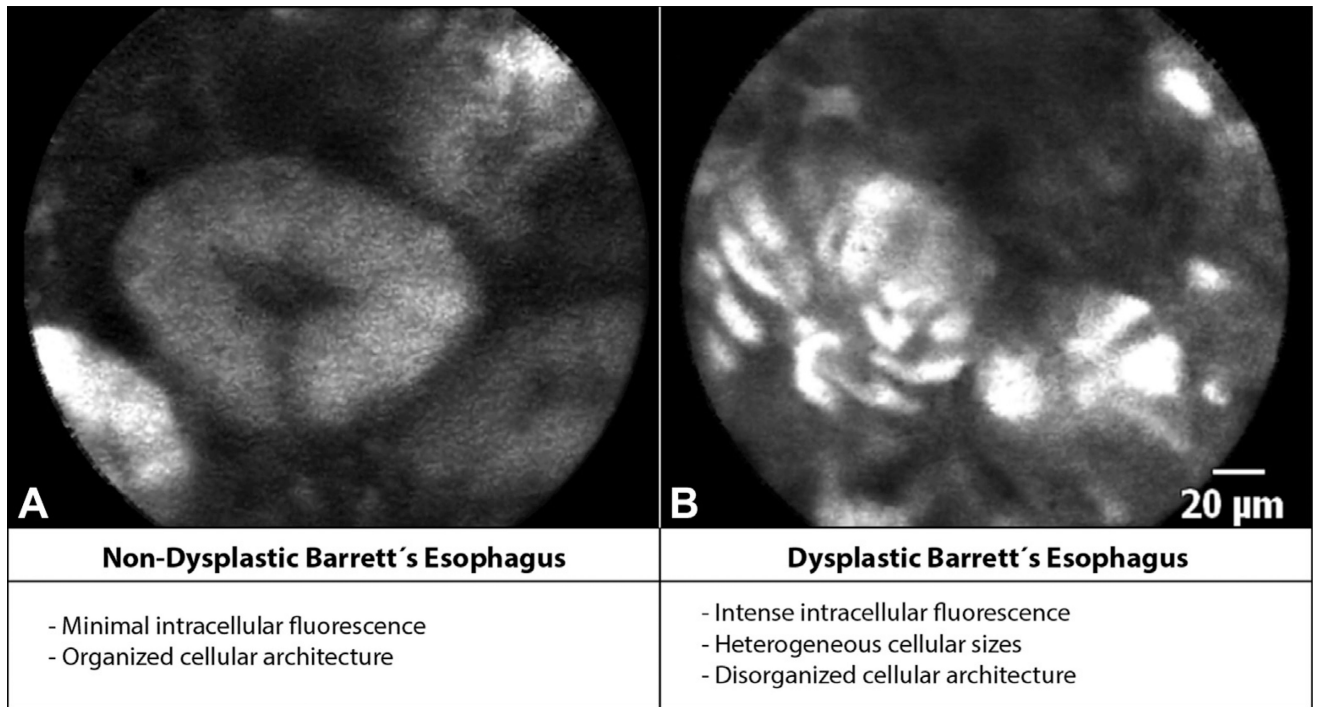
Figure 2.
Probe confocal laser endomicroscopy (pCLE) fluorescence criteria. **A**, pCLE images of nondysplastic Barrett's esophagus (BE) showing minimal intracellular fluorescence and organized cellular architecture. **B**, Dysplastic BE showing intense intracellular fluorescence with heterogeneous cellular sizes and disorganized cellular architecture based on the pCLE fluorescence criteria.
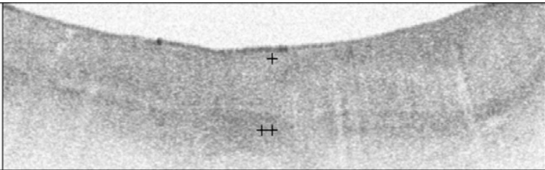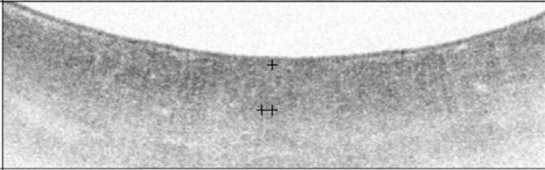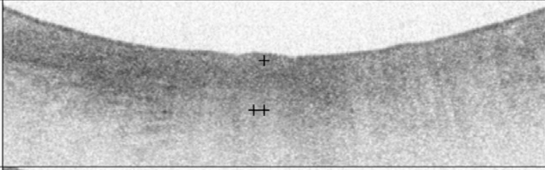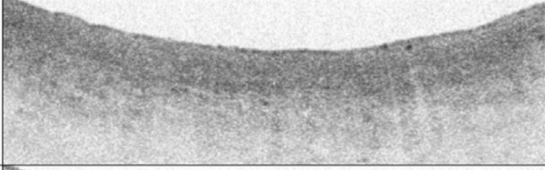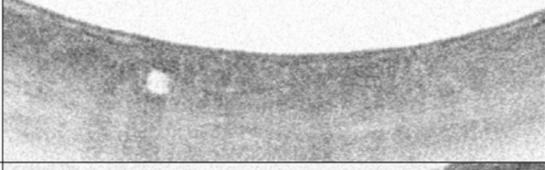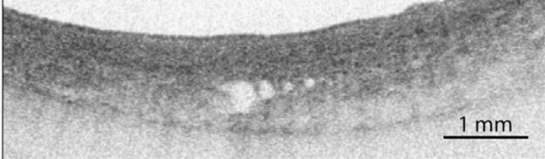
Figure 3.
The volumetric laser endomicroscopy scoring index (OCT-SI) is used to diagnose Barrett's esophagus (BE)-associated dysplasia. The scoring index consists of 2 independent criteria (surface-to-subsurface signal intensity and glandular architecture) that are added to calculate a dysplasia score. A dysplasia score of 2 is associated with a sensitivity of 83% and a specificity of 75% for the diagnosis of neoplasia in BE by using optical coherence tomography. The volumetric laser endomicroscopy surface signal intensity is represented by + and the subsurface intensity by ++. Glandular atypia is defined by the presence of irregular and/or dilated glands.
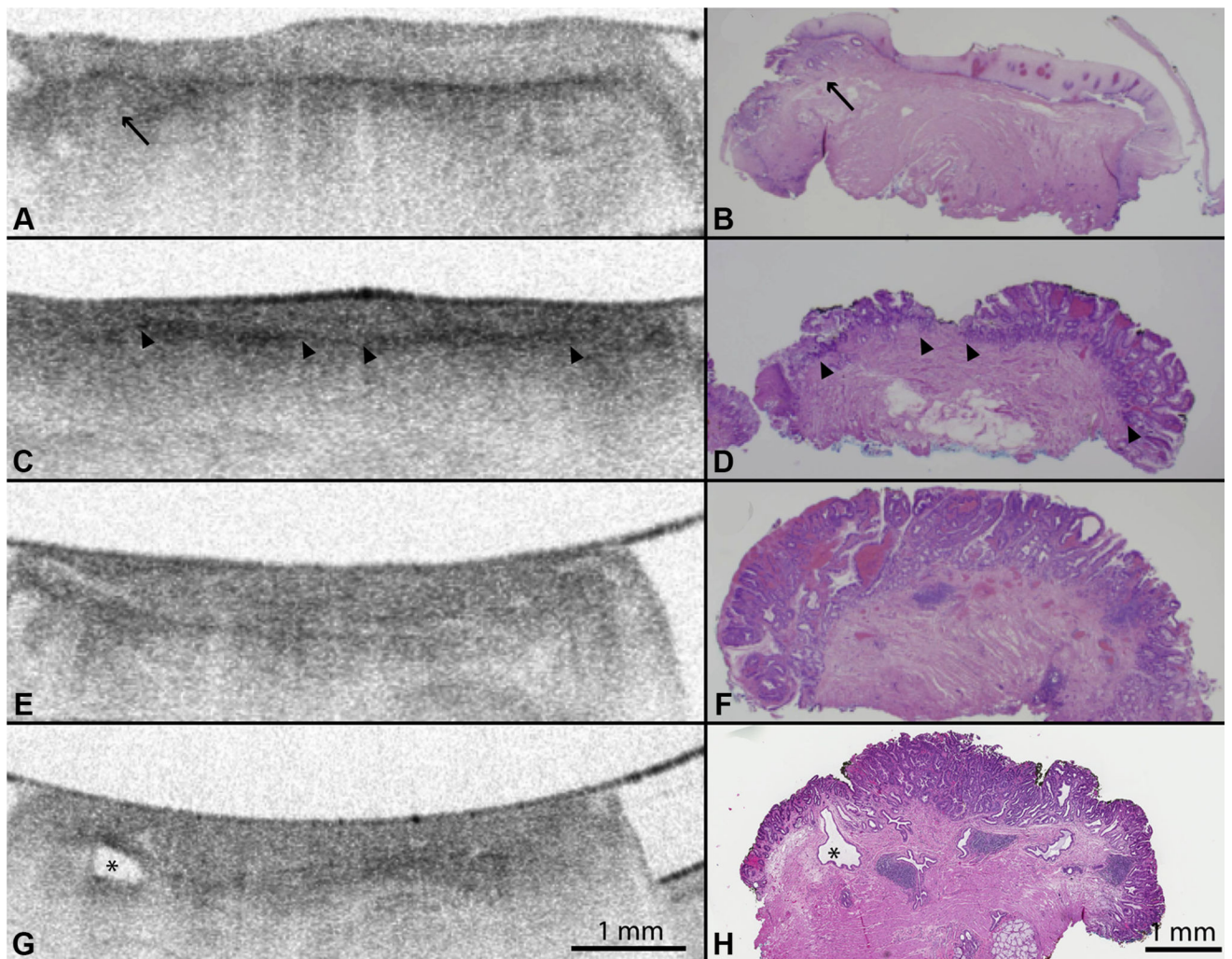
Figure 4.
A, Volumetric laser endomicroscopy (VLE) imaging of EMR specimens with confirmed **B**, histopathology showing layered mucosal architecture of squamous epithelium (H&E, orig. mag. × 15). *Black arrow* shows a small focus of subsquamous Barrett's esophagus (BE). **C, D**, VLE images of histopathology confirmed nondysplastic BE showing loss of layered mucosal architecture and partial effacement of the mucosal layer (>2-mm layer). The partial effacement of the VLE mucosal layer shows less distinction between mucosa and submucosa compared with squamous epithelium (*arrowheads*). **E**, VLE images of BE with high-grade dysplasia confirmed by **F**, histology showing loss of layered mucosal architecture and complete effacement of the mucosal layer (<2-mm layer). **G**, VLE images of histologically confirmed high-grade dysplasia showing an atypical glandular structure that represents a dilated submucosal duct (as noted by the *asterisk*).
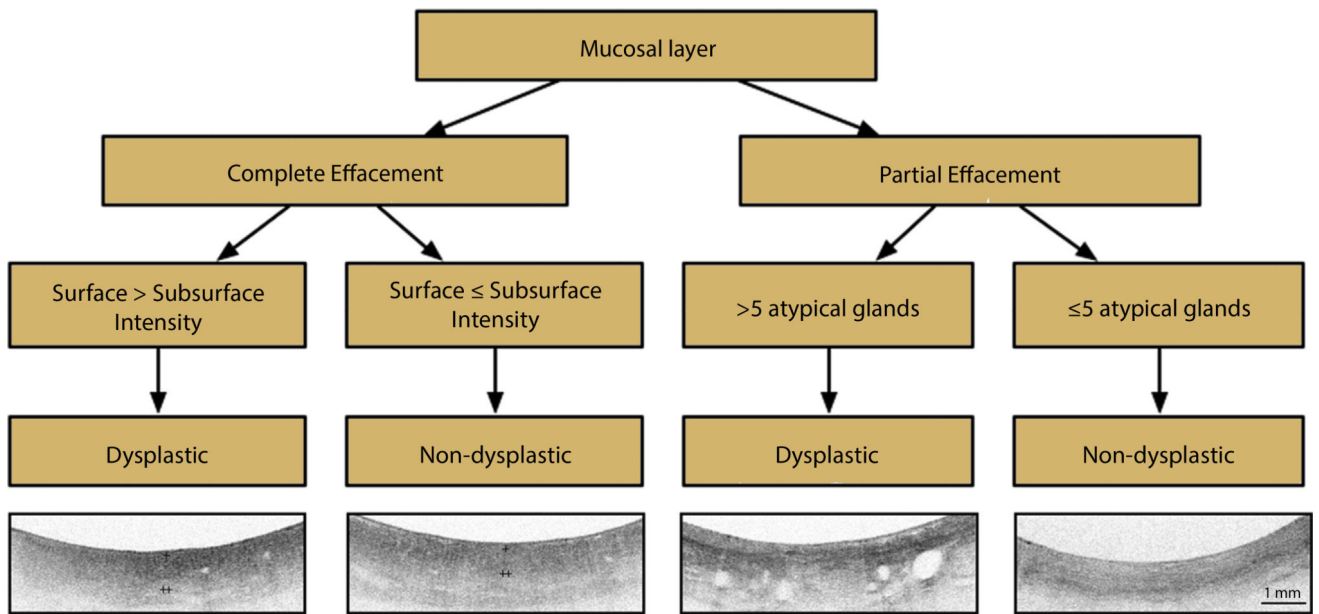
Figure 5.
Volumetric laser endomicroscopy diagnostic algorithm (VLE-DA). Interpretation of the VLE-DA is performed over a longitudinal distance of 1 cm of Barrett's esophagus (BE). Partial effacement of the mucosal layer is defined by a mucosal layer 2 mm in transverse cross-section present in 50% of the scan. Complete effacement of the mucosal layer is defined by the presence of a mucosal layer over <50% of the scan. A rating of image surface-to-subsurface intensity corresponds to the most prevalent ratio (surface > subsurface intensity vs surface < subsurface intensity) present in 50% of the scan. The VLE surface signal intensity is represented by + and subsurface intensity by ++.
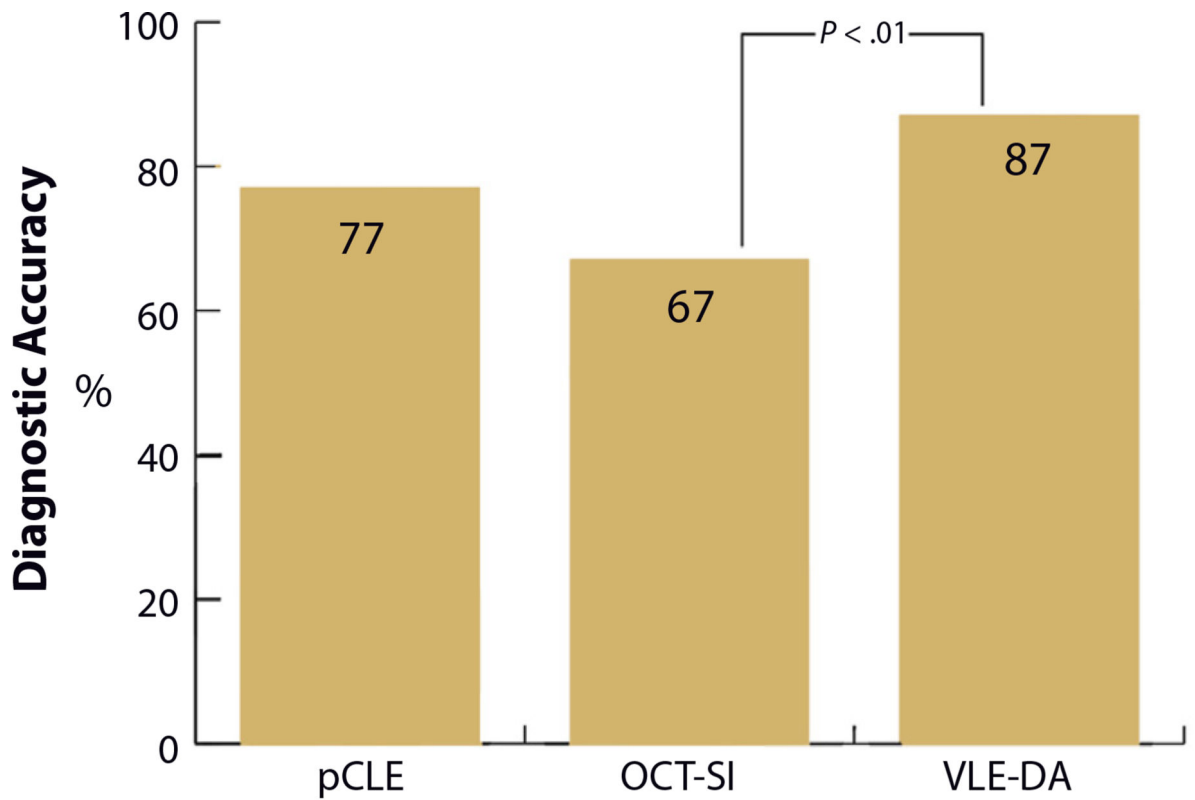
	Sensitivity (95% CI)	Specificity (95% CI)	PPV (95% CI)	NPV (95% CI)
pCLE	76 (59-88)	79 (53-92)	89 (72-96)	63 (39-82)
OCT-SI	70 (52-84)	60 (36-79)	80 (62-90)	47 (26-70)
VLE-DA	86 (69-96)	88 (60-99)	94 (77-98)	75 (50-91)

Figure 6.
A, Graph showing diagnostic accuracy of point confocal laser endomicroscopy compared with volumetric laser endomicroscopy (VLE) by using the VLE scoring index (OCT-SI) at a diagnostic threshold of 3 and the diagnostic algorithm. An OCT-SI threshold of 3 showed improved diagnostic characteristics compared with other thresholds on post hoc analysis. **B**, Table showing sensitivity and specificity of pCLE, OCT-SI, and VLE-DA. *pCLE*, probe confocal laser endomicroscopy; *OCT-SI*, VLE scoring index; *VLE-DA*, volumetric laser endomicroscopy diagnostic algorithm; *CI*, confidence interval; *PPV*, positive predictive value; *NPV*, negative predictive value.

TABLE 1

Baseline characteristics

Patient characteristic (N = 27)	
Age, mean (± SD)	72 (10)
Male sex, no. (%)	24 (89)
RFA-treated patients, no. (%)	6(22)
Time from RFA to EMR, mean (range), mo	8.9 (2.6–16.6)
EMR specimen characteristic (N = 50)	
Length, mean (± SD)	0.9 (0.2)
EMR specimens from RFA-treated patients, no. (%)	9 (18)
Nonneoplastic	16 (32)
Nondysplastic Barrett's esophagus	10 (20)
Low-grade dysplasia	6(12)
Neoplastic	34 (68)
High-grade dysplasia	24 (48)
Intramucosal adenocarcinoma	10 (20)

SD, Standard deviation; *RFA*, radio frequency ablation.